Mechatronics 78 (2021) 102631

Contents lists available at ScienceDirect

Mechatronics

journal homepage: www.elsevier.com/locate/mechatronics

Self-sensing control of resonant MEMS scanner by comb-drive current feedback☆

David Brunner [a,*], Stephan Albert [b], Marcus Hennecke [c], Franz Darrer [c], Georg Schitter [a]

[a] TU Wien, Automation and Control Institute (ACIN), Gusshausstrasse 27-29, 1040 Vienna, Austria
[b] Infineon Technologies AG, Neubiberg, Germany
[c] Infineon Technologies Austria AG, Graz, Austria

ARTICLE INFO

Keywords:
Micro-electro-mechanical system (MEMS)
Nonlinear systems
Phase locked loop (PLL)
Precision control
Resonant scanning mirror
Self-sensing

ABSTRACT

This paper proposes a novel self-sensing control concept for resonant MEMS mirrors solely based on the comb-drive current generated by the mirror movement and simple circuitry. Phase errors are immediately compensated by asynchronous switching of the driving voltage using the precise zero crossing detection by the steep current gradient. The mirror amplitude is detected based on the time difference between a comparator threshold crossing of the current signal and the zero crossing of the mirror, while it is controlled by the duty cycle of the driving voltage signal. The proper threshold setting is analyzed regarding the obtained sensitivity and uncertainty of the amplitude detection and is verified by measurements. It is found that even for symmetric out-of-plane comb-drives the scanning direction can be determined utilizing the mode coupling phenomenon of a lightweight MEMS mirror design with reinforcement structure. Experiments show that the proposed control concept results in a low optical pointing uncertainty of 0.52 mdeg, which allows 10 000 pixels with a precision of 10 sigma at a scanning frequency of 2 kHz. Thus a lightweight and simple design of a high performance MEMS mirror is precisely controlled in its oscillation without any additional sensors or complex circuitry.

1. Introduction

Resonant micro-electro-mechanical system (MEMS) mirrors receive much attention in high precision scanning systems. They achieve large deflection angles at frequencies of several kilohertz while their power consumption is low due to a high Q-factor. The small form factor and the manufacturing with standard CMOS technology on a silicon wafer allow easy and cheap mass production. MEMS mirrors have been studied and applied for several applications such as in pico-projectors [1], optical coherence tomography [2] and automotive lidar [3–5]. In order to maintain the scanning trajectory even if environmental conditions change a phase locked loop (PLL) is applied [6]. As resonant electrostatic MEMS mirrors usually operate in parametric resonance [7] it is hard to analyze the closed loop performance and to guarantee accurate pixel synchronization for various MEMS mirror designs. Therefore precise angle feedback is necessary to track the mirror movement. Various sensing methods are proposed in literature, such as piezoresistive [8], piezoelectric [9], acoustic [10], optical [6] and capacitive [11,12]. Piezoresistive and piezoelectric sensing are subject of extensive research and provide continuous angle feedback, but require additional processing steps and suffer from durability and degradation problems as well as temperature dependencies. Angle feedback based on emitted acoustic waves may not be applicable for harsh environments such as in industrial or automotive applications. The trajectory of resonant MEMS mirrors is mainly determined by the spring suspension as the Q-factor is usually high, which allows a trajectory reconstruction solely from amplitude and frequency or phase measurements. An optical sensing method variant based on the timings of two photo diodes at the backside of the mirror shows good amplitude and phase detection performance even at large ambient temperature variation [6]. However optical components are required close to the MEMS mirror and the precision might be influenced by scattered light from the main light path at the front side. The capacitive sensing methods use a modulated high frequency carrier or a charge integrator to extract the amplitude and phase from the angle dependent comb-drive capacitance. Hence, these methods represent a self-sensing concept as the same comb-drives are used for sensing as for actuation and no additional components or manufacturing processes are necessary at the mirror. However the proposed capacitive methods are rather complex and do not provide a

☆ This paper was recommended for publication by Associate Editor Micky Rakotondrabe.

* Corresponding author.
E-mail addresses: brunner@acin.tuwien.ac.at (D. Brunner), StephanGerhard.Albert@infineon.com (S. Albert), Marcus.Hennecke@infineon.com (M. Hennecke), Franz.Darrer@infineon.com (F. Darrer), schitter@acin.tuwien.ac.at (G. Schitter).

https://doi.org/10.1016/j.mechatronics.2021.102631
Received 2 February 2021; Received in revised form 8 May 2021; Accepted 19 July 2021
Available online 2 August 2021

high SNR measurement of the amplitude as the capacitance change is low when the comb-drives are fully disengaged, i.e. at large deflection, and small amplitude variations are hard to discriminate. Furthermore for the typical case where the comb movement is out-of-plane and the stator as well as the rotor combs are of the same silicon layer, the scanning direction cannot be determined due to the symmetry of the capacitance for positive and negative angles. However in applications such as automotive lidar the knowledge of the scanning direction at any time is crucial as otherwise the perceived data is unreliable and may lead to potentially hazardous situations. To overcome this problem an additional sensor or an asymmetric comb-drive design such as staggered or angular vertical combs [13] are usually necessary. Hence, there is no method yet that allows a simple and precise full-self sensing control implementation for electrostatic resonant MEMS mirrors without introducing an asymmetry by design or additional sensors.

The contribution of this paper is the extended digital asynchronous PLL (eDAsPLL) enabling fast and high precision control of resonant MEMS mirrors solely based on comb-drive current feedback. This paper extends the phase control concept of the DAsPLL presented in [14] with a precise amplitude detection and control as well as a direction detection concept for MEMS mirrors with single-layer out-of-plane comb-drives. The amplitude detection method using simple comparators is analyzed based on a simplified mirror model to obtain the highest performance with respect to sensitivity and noise influence. The scanning direction is detected by the difference of the left and the right side comb-drive current signals caused by a mode coupling phenomenon of lightweight MEMS mirror designs with reinforcement structures. All proposed methods use self-sensing concepts and do not require any additional component at the proximity of the mirror nor a complex circuitry.

The paper is organized as follows. Section 2 describes the used MEMS mirror including the mode coupling as well as the driving and sensing circuitry. In Section 3 the phase control concept is summarized and extended by the amplitude control and the direction detection concepts. Section 4 provides the experimental verification of the proposed methods. In Section 5 the paper is concluded.

2. System description

2.1. MEMS mirror

Fig. 1 shows the investigated MEMS mirror with out-of-plane comb-drives and a combined suspension using torsion bars and leaf springs for improved undesired mode suppression. This mirror exhibits additionally to the inherently nonlinear actuation principle a nonlinear damping and a hardening spring as shown in [15]. The comb-drive capacitance curve is given in Fig. 2, which is symmetric regarding the rotation angle and maximum when the mirror is at rest. The mechanism thanks to which such MEMS mirrors are able to oscillate is called parametric resonance, which results in highly nonlinear frequency responses [7]. One characteristic of this phenomenon is that for the most efficient actuation the driving frequency has to be twice the mirror oscillation frequency achieving first-order parametric resonance.

For improving the MEMS mirror performance by increasing scanning frequency and aperture size, dynamic deformation is one of the main limiting factors [16]. A possible solution is to use reinforcement structures on the backside of a thin mirror that make the mirror lightweight while still dynamically flat [3,17,18]. As a consequence the thicker reinforcement layer shifts the center of mass away from the rotation axis, whose out-of-plane position is mainly determined by the thinner suspensions. This means that the MEMS scanner acquires a rotating unbalance. A reinforcement structure at the backside of the mirror significantly improves the performance but also causes a mode coupling between the intended rotational mode R_X and the in-plane

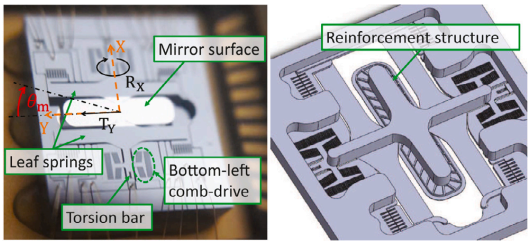

Fig. 1. Picture and definitions of the used MEMS mirror with out-of-plane comb-drives and an aperture size of 3.2×0.8 mm^2. The rotor suspension consists of the conventional torsion bars and additional leaf springs. For clarity the bottom-left (BL) comb-drive is shown. The lightweight mirror has reinforcement structures on the backside to prevent dynamic deformations.

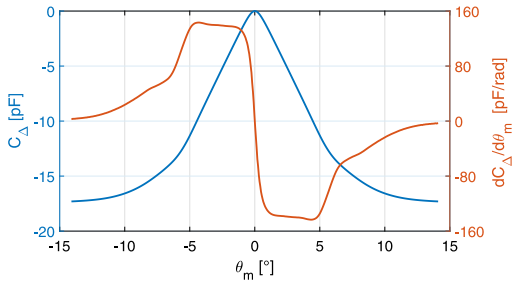

Fig. 2. Measured comb-drive capacitance curve and its derivative with respect to the mirror rotation angle obtained by an actuated decay measurement [15]. The capacitance shows a triangular shape and is symmetric regarding zero angle. The zero angle capacitance cannot be estimated by the method proposed in [15] and is therefore arbitrarily set to zero.

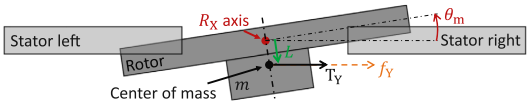

Fig. 3. Principal model of the mode coupling due to the mismatch of the center of mass and the rotation axis.

translational mode in Y direction T_Y. The coupling force f_Y originates from the Euler force and can be written as

$$f_Y = -m\,L\,\cos\left(\theta_m\right)\,\ddot{\theta}_m\,, \tag{1}$$

where θ_m is the rotation angle, m is the rotor mass and L is the distance between center of mass and the rotational axis as depicted in Fig. 3. As the used MEMS mirror is designed for rotation angles of about ±15° the cosine term in (1) can be approximated by $\cos\left(\theta_m\right) \approx 1$. Therefore the T_Y mode is mainly actuated with the frequency content of R_X which requires a good mode separation by design. Usually MEMS mirrors are designed to have their parasitic modes way above the desired rotational mode leading to only a small T_Y movement by the coupling due to the higher stiffness. Additionally the analysis of strong disturbances such as external vibrations studied in [19] show that a quick remedy is to design the R_X resonance above the maximum expected vibration frequency to avoid the main coupling. The used MEMS mirror is targeted for a line-scan lidar as described in [4,5] and has its rotational mode at 1.85 kHz, while the translational Y mode is at 9.95 kHz.

Published version of the article: D. Brunner, S. Albert, F. Darrer, M. Hennecke, and G. Schitter, "Self-sensing control of resonant MEMS scanner by comb-drive current feedback", *Mechatronics*, vol. 78, 102631, 2021. DOI: 10.1016/j.mechatronics.2021.102631

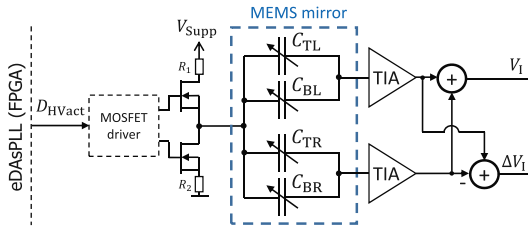

Fig. 4. Driving and sensing circuitry for a comb actuated resonant MEMS mirror. The rotor potential can be switched by D_{HVact}. The stator combs are separated into left and right side and connected to TIAs to measure the generated displacement current. The TIAs have a gain G_{TIA} of 45.16 $\frac{V}{mA}$ and a bandwidth of 270 kHz.

2.2. Driving and sensing circuitry

The circuitry used for driving and sensing the MEMS mirror is shown in Fig. 4, where the comb-drives are modeled as variable capacitors. A single bit digital signal D_{HVact} controls the rotor potential via a MOSFET half-bridge. The individually accessible stator combs are separated into left and right side and connected to transimpedance amplifiers (TIA) to measure the comb-drive current, i.e.

$$I_C = V_{Supp} \frac{dC(\theta_m)}{d\theta_m} \dot{\theta}_m + C(\theta_m) \frac{dV_{Supp}}{dt}, \quad (2)$$

which consists of the displacement current generated by the mirror movement and the measurement noise originating from supply voltage changes. The TIA outputs are both summed and subtracted in order to allow the detection of phase, amplitude and scanning direction by the methods presented in the next section.

3. MEMS mirror control design

3.1. Phase control

The DAsPLL concept proposed in [14] uses the summed current signal V_I and two comparators with the thresholds V_C and V_{ZC} for reliably detecting the zero crossing of the mirror with high precision. Due to the triangular shape of the comb-drive capacitance, the summed current signal shows a sharp zero crossing when the mirror passes zero angle. Hence, a zero crossing is detected if both comparators are crossed successively in time in the correct order. The driving signal is switched off asynchronously to the FPGA clock by passing the zero crossing comparator signal D_{ZC} directly to the driving output D_{HVact}. After a quarter mirror period the driving signal is switched on again, resulting in first-order parametric resonance with zero phase and 50% duty cycle.

The DAsPLL concept is fundamentally different from a conventional PLL design, where the PLL period is adjusted according to the measured phase errors between mirror oscillation and the PLL. A stability analysis based on a linearized model of the used MEMS mirror operated by a conventional PLL utilizing a PI control law is given in [20]. In contrast, the DAsPLL generates a driving signal directly linked to the MEMS mirror movement, which allows fast tracking of the mirror oscillation and immediate phase compensation. High precision laser synchronization is achieved with an optical pointing uncertainty of 0.3 mdeg at the center of a 57.5° field of view (FoV) as reported in [14]. However as only the phase is detected, there is no information about the oscillation amplitude or the scanning direction.

3.2. Amplitude detection and control

Amplitude detection and control is crucial as a constant FoV has to be guaranteed during operation. As the DAsPLL keeps zero phase with a fixed duty cycle, the mirror amplitude will vary at changing environmental conditions [6], i.e. changing the FoV. There are two possibilities for controlling the amplitude, either adjusting the supply voltage V_{Supp} [6] or the duty cycle [21] of the driving signal. As fast control requires a large bandwidth, the supply voltage control would increase the detection noise due to the differentiating behavior of the driving voltage to the comb-drive current (see (2)), which is not desirable. Therefore, and due to the easier implementation, t_{on}, which defines the switching on delay of the driving voltage after a detected zero crossing is used to control the mirror amplitude. This concept is similar to the duty cycle control, while zero phase is kept, i.e. the switching off of the driving voltage coincides with the mirror zero crossing at any time. Control margin can be secured by using a duty cycle smaller or larger than 50%. However an increased duty cycle provides a longer time period where the driving voltage is on and the displacement current can be measured. Fig. 6 shows an operation point with 77% duty cycle, providing a reasonable control margin.

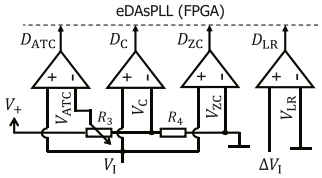

Fig. 5. Circuitry for phase, amplitude and direction detection consisting of four comparators and one voltage divider. The digital output signals of the comparators are directly connected to the FPGA pins where the eDAsPLL is implemented. The signals D_C and D_{ZC} are used for phase detection, D_{ATC} and D_{ZC} for amplitude detection and D_{LR} for direction detection.

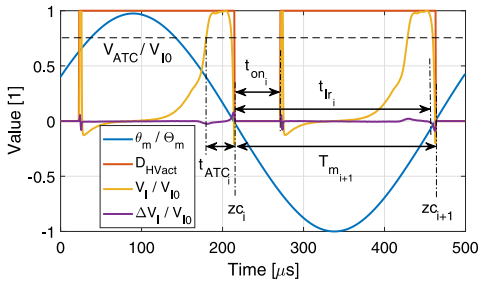

Fig. 6. Definitions and measured signals at the used operation point (Θ_m = 13.75°, 77% duty cycle, V_{Supp} = 76 V, V_{I0} = 1.377 V). The mirror trajectory is measured using a position sensitive detector (PSD) [4]. At a detected zero crossing (zc) the mirror half period T_m is measured and the delays t_{on} and t_{lr} are calculated for amplitude control and direction detection respectively. The sharp peaks in the summed current signal V_I are due to the fast driving voltage switching.

The simple amplitude detection method proposed in this study is based on the timing between two comparator threshold crossings, i.e. V_{ATC} and V_{ZC}, of the summed current signal V_I. Fig. 5 shows the simple detection circuitry used in this study. Because a time difference is effectively controlled, this concept is called amplitude timing control (ATC) in this paper.

3.2.1. Detection concept

Assuming a constant supply voltage V_{Supp} in (2) and the mirror zero crossing happening at $t = 0$, the condition for the crossing of V_{ATC} can be expressed as

$$\frac{V_{ATC}}{G_{TIA}} = V_{Supp} \frac{dC_\Delta\left(\theta_m\big|_{t=-t_{ATC}}\right)}{d\theta_m} \dot{\theta}_m\big|_{t=-t_{ATC}}, \quad (3)$$

Published version of the article: D. Brunner, S. Albert, F. Darrer, M. Hennecke, and G. Schitter, "Self-sensing control of resonant MEMS scanner by comb-drive current feedback", *Mechatronics*, vol. 78, 102631, 2021. DOI: 10.1016/j.mechatronics.2021.102631

which represents a highly nonlinear relation with the comb-drive capacitance curve in Fig. 2. In order to judge the usability of a specific threshold voltage V_{ATC}, the sensitivity, i.e.

$$S = \frac{\mathrm{d}\, t_{\mathrm{ATC}}}{\mathrm{d}\, \Theta_{\mathrm{m}}}, \tag{4}$$

(3) has to be analyzed regarding amplitude changes. However not only the sensitivity but also the uncertainty of the amplitude detection is of interest, as fast controllers need a high precision sensing. The precision of the detection signal depends on the local current gradient at the threshold crossing, which can be expressed as

$$\frac{\mathrm{d}I_{\mathrm{C}}}{\mathrm{d}\, t} = V_{\mathrm{Supp}} \left[\frac{\mathrm{d}^2 C_{\Delta}\left(\theta_{\mathrm{m}}\right)}{\mathrm{d}\theta_{\mathrm{m}}^2} \dot{\theta}_{\mathrm{m}}^2 + \frac{\mathrm{d}C_{\Delta}\left(\theta_{\mathrm{m}}\right)}{\mathrm{d}\theta_{\mathrm{m}}} \ddot{\theta}_{\mathrm{m}} \right]. \tag{5}$$

Due to the high steepness of the current at the zero crossing, the uncertainty is mainly determined by the crossing of V_{ATC}. Therefore, the uncertainty of the amplitude detection originating from noise on the current signal is

$$U = \frac{\mathrm{d}\, \Theta_{\mathrm{m}}}{\mathrm{d}\, t_{\mathrm{ATC}}} \frac{\mathrm{d}\, t}{\mathrm{d}I_{\mathrm{C}}}\bigg|_{t=-t_{\mathrm{ATC}}} = \frac{1}{S} \frac{\mathrm{d}\, t}{\mathrm{d}I_{\mathrm{C}}}\bigg|_{t=-t_{\mathrm{ATC}}}. \tag{6}$$

In order to calculate (4) and (6) for different thresholds and operation points, the mirror angle, velocity and acceleration at the crossing of V_{ATC} are necessary. For simplicity the MEMS mirror can be modeled as a conservative system with the equation of motion

$$\ddot{\theta}_{\mathrm{m}} + k_{\mathrm{n}}\left(\theta_{\mathrm{m}}\right) \theta_{\mathrm{m}} = 0, \tag{7}$$

where $k_{\mathrm{n}}\left(\theta_{\mathrm{m}}\right)$ is the normalized nonlinear spring stiffness obtained by a decay measurement (see [15]). This approximation is valid as the quality factor of such MEMS mirrors is usually high and is larger than 160 for this specific design. The velocity can then be calculated by the energy conservation law since the sum of the kinetic and the potential energy have to be constant and equal to the total system energy, i.e.

$$\overbrace{\frac{1}{2}\dot{\theta}_{\mathrm{m}}^2}^{\text{kinetic energy}} + \overbrace{\int_0^{\theta_{\mathrm{m}}} k_n\left(\theta_{\mathrm{m}}\right) \theta_{\mathrm{m}}\, \mathrm{d}\theta_{\mathrm{m}}}^{\text{potential energy}} = \overbrace{\int_0^{\Theta_{\mathrm{m}}} k_n\left(\theta_{\mathrm{m}}\right) \theta_{\mathrm{m}}\, \mathrm{d}\theta_{\mathrm{m}}}^{\text{total energy}}. \tag{8}$$

Therefore, the mirror velocity can be expressed as

$$\dot{\theta}_{\mathrm{m}} = \sqrt{2} \sqrt{\int_{\theta_{\mathrm{m}}}^{\Theta_{\mathrm{m}}} k_{\mathrm{n}}\left(\theta_{\mathrm{m}}\right) \theta_{\mathrm{m}}\, \mathrm{d}\theta_{\mathrm{m}}}, \tag{9}$$

which only depends on the mirror angle and amplitude. Subsequently, t_{ATC} can be calculated by simple integration of the inverse mirror velocity until the condition (3) is fulfilled. The sensitivity can then be easily obtained by slightly varying the amplitude. The uncertainty can be calculated by evaluating (6) using (5), (7) and (9) and the corresponding sensitivity. By this the trade-offs between sensitivity and uncertainty can be analyzed. The obtained values are given in Section 4.2 together with the experimental results.

The presented detection concept analysis is also applicable for other electrostatic resonant MEMS mirror designs and allows the evaluation of the amplitude detection performance already during the design phase. This knowledge provides quantitative values for the hardware selection, such as required timing resolution, TIA gain settings and filters, without the necessity of an actual manufactured and operational MEMS mirror.

3.2.2. Control concept

A block diagram of the amplitude control loop is shown in Fig. 7, which is executed at each detected zero crossing, where new mirror amplitude and period measurements are available. In this study, a simple PI approach is used to control the mirror amplitude by the measured amplitude timing value deviation from its desired value. The PI control law is therefore given by

$$t_{\mathrm{on}_i} = \frac{1}{2}\hat{T}_{\mathrm{m}_i} - G_{\mathrm{P}}\left(\bar{t}_{\mathrm{ATC}} - t_{\mathrm{ATC}_i}\right) - G_{\mathrm{I}} \sum_{j=-\infty}^{i} \left(\bar{t}_{\mathrm{ATC}} - t_{\mathrm{ATC}_j}\right), \tag{10}$$

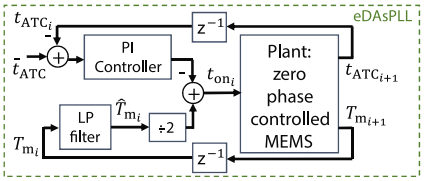

Fig. 7. Block diagram of the amplitude control loop executed at each detected zero crossing. The plant represents the MEMS mirror operated in zero phase. The measured periods are low pass filtered, divided by 2 and added to the PI controlled amplitude errors to obtain the switching on delay.

where $\bar{t}_{\mathrm{ATC}}$ is the set-point time corresponding to the desired amplitude and G_{P} and G_{I} are the P and I gains, respectively. Appropriate gain settings can be derived by the nonlinear mirror model in [15] or by a linearization of the nominal operation point similar as in [20]. If the amplitude controller is turned off, i.e. $G_{\mathrm{I}} = G_{\mathrm{P}} = 0$, the eDAsPLL degenerates to the DAsPLL with 50% duty cycle according to (10).

In order to cope with measurement noise the mirror half period is filtered using a first order low-pass, i.e.

$$\hat{T}_{\mathrm{m}_i} = \hat{T}_{\mathrm{m}_{i-1}} + G_{\mathrm{LP}}\left(T_{\mathrm{m}_i} - \hat{T}_{\mathrm{m}_{i-1}}\right), \tag{11}$$

where $0 \leq G_{\mathrm{LP}} \leq 1$ is the filter gain. A low filter gain is preferred for noise suppression while a too low gain can cause dynamic effects on the amplitude control loop.

It has to be noted that for the used MEMS mirror the operation points with zero phase and duty cycles larger than 50%, as in Fig. 6, are unstable in open loop, but can be maintained by the immediate phase compensation of the DAsPLL. Therefore, the DAsPLL and consequently also the eDAsPLL can properly operate MEMS mirrors exhibiting both softening or hardening behavior in open loop stable or unstable regions, while their implementation is simple. This comes with the drawback that excessive noise on the mirror zero crossing detection directly influences the jitter of the driving signal, which necessities additional filtering methods to obtain a stable laser synchronization.

3.3. Detection of scanning direction

Capacitive sensing methods with single-layer out-of-plane comb-drives usually have difficulties to determine the scanning direction as the capacitance variation is the same for positive and negative angles. In this section we propose a direction detection exploiting the coupling to a parasitic translational mode for lightweight MEMS mirrors with reinforcement structures. Fig. 8 shows zoomed graphs at the mirror zero crossings in Fig. 6. As the $\mathrm{T_Y}$ mode is actuated by the mirror's rotational mode, an asymmetry is obtained, which results in a difference of the right and the left comb-drive current signals. The measured difference current ΔV_{I} shows distinct peaks at the zero crossings of the mirror with positive or negative voltage depending on the mirror movement direction. These peaks happen as the $\mathrm{T_Y}$ mode is actuated by a frequency well below its resonance, where the displacement is in phase with the actuation force f_{Y} and due to (1) also with the rotation angle. This causes an increase in the left side comb-drive capacitance and a decrease in the right side, when the mirror changes from positive to negative angles, leading to a positive peak in the difference current. Therefore, a simple method to detect the scanning direction is to use a comparator with a threshold voltage V_{LR} at zero volt to evaluate the sign of the peaks. A robust concept is to count an FPGA register up or down whenever the comparator output is high or low, respectively and to read the register at the end of the evaluation window. As the evaluation window should be limited to a reasonable time span close to the zero crossing, the starting time is arbitrarily defined by

$$t_{\mathrm{lr}_i} = \left(1 - 2^{-6}\right) \hat{T}_{\mathrm{m}_i}, \tag{12}$$

Published version of the article: D. Brunner, S. Albert, F. Darrer, M. Hennecke, and G. Schitter, "Self-sensing control of resonant MEMS scanner by comb-drive current feedback", *Mechatronics*, vol. 78, 102631, 2021. DOI: 10.1016/j.mechatronics.2021.102631

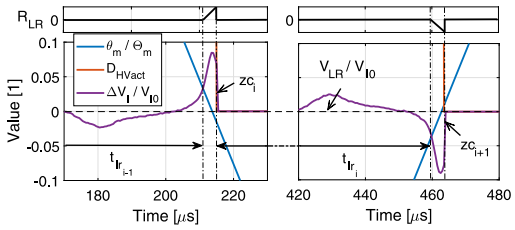

Fig. 8. Signals and definitions used for direction detection zoomed from Fig. 6. The subtraction of the left and the right current signals provides distinct peaks whose sign depend on the zero crossing direction. During the evaluation window defined by t_{lr} and the following zero crossing, the FPGA register $\mathrm{R_{LR}}$ counts up or down whenever the comparator output D_{LR} is high or low respectively.

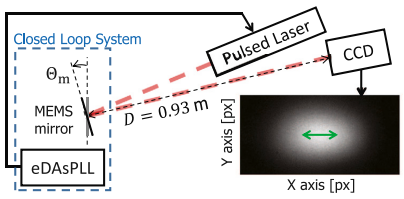

Fig. 9. Setup for optical evaluation of the proposed amplitude control concept. A pulsed laser is triggered by the eDAsPLL, when the mirror is expected to be at maximum deflection and reflected towards a CCD at a distance D. The CCD frames contain only single laser pulses and provide a precise measurement of the amplitude error by analyzing the spot movement frame by frame indicated by the green double arrow. (For interpretation of the references to color in this figure legend, the reader is referred to the web version of this article.)

while it ends at the next detected zero crossing, i.e. zc_{i+1}.

For the proposed method even a quite weak coupling is sufficient to generate a distinguishable difference current. Thus a strong parasitic mode suppression by design is compatible with the method such that the scanner's operational robustness is not compromised. Following this, it is expected that the method is also applicable for MEMS mirror designs with lower or higher scanning frequency provided that the $\mathrm{T_Y}$ mode is sufficiently higher than the $\mathrm{R_X}$, which is the typical case.

4. Experimental results

4.1. Experimental setup

As MEMS mirrors are intended to be used in high precision scanning and projection systems, both the trajectory stability and the precision of the pixel synchronization are of importance. Hence, the setup in Fig. 9 is developed. The closed loop system comprises the eDAsPLL implemented on an FPGA (Zedboard, 100 MHz, Digilent, Pullman, WA, US), the driving and sensing circuits and the MEMS mirror. A pulsed laser is triggered, when the mirror is expected to be at maximum deflection, i.e. Θ_{m}, which is a quarter mirror period after a detected zero crossing. The pulse gets reflected by the MEMS mirror and hits the CCD, where the exposure time is adjusted such that each captured frame contains only a single laser pulse. The obtained frame to frame spot movement can be analyzed to calculate the mirror amplitude error, i.e.

$$\Delta\Theta_{\mathrm{m}} = \frac{1}{2}\tan^{-1}\left(\frac{\Delta r_{\mathrm{CCD}}}{D}\right), \tag{13}$$

where Δr_{CCD} is the spot movement on the CCD relative to the mean position with 90° incidence angle and D is the distance between the MEMS mirror and the CCD. Therefore, a large distance provides a high resolution measurement of the amplitude errors.

4.2. Verification of amplitude detection analysis

In this section, the analysis in Section 3.2 is verified by measurements. First, the ATC is turned off at nominal amplitude operation and the threshold voltage V_{ATC} is varied to obtain the amplitude timing values t_{ATC}, as shown in Fig. 10, which are in good agreement with the proposed model. The deviations at low threshold voltages are due to model errors, but also due to the low gradient and finite curvature of the current signal at the threshold crossing, which leads to a shift of the average value by noise. Therefore, the shift depends on the noise level, which is not desirable if the system is intended to operate in unknown environments with varying noise influences.

If the ATC mode is turned on the sensitivity can be obtained by measuring the mean amplitude change at an amplitude timing set-point step. Fig. 11 shows the sensitivity over the threshold voltage,

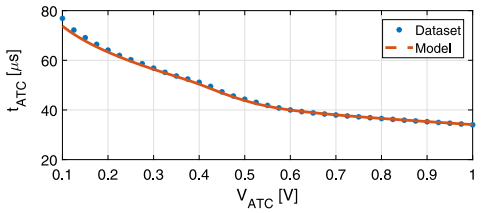

Fig. 10. Measured average t_{ATC} when the ATC is turned off and theoretical model over threshold voltage ($\Theta_{\mathrm{m}} = 13.75°$, $V_{\mathrm{Supp}} = 76$ V). Only at low threshold voltages a slight deviation from the model is observed.

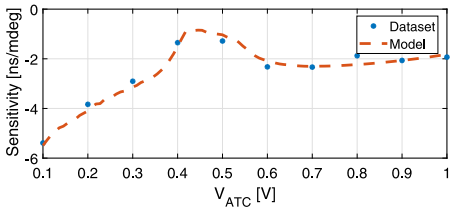

Fig. 11. Measured sensitivity obtained by analyzing the CCD frames at an amplitude timing set-point step of 50 ns and the proposed model.

which again agrees well with the predicted behavior. It reveals that for threshold voltages smaller than 0.35 V the amplitude detection sensitivity increases up to −5.5 ns/mdeg, while higher voltages achieve only about −2 ns/mdeg.

Assuming a Gaussian additive noise on the current signal with a standard deviation σ_{I}, the uncertainty of the amplitude detection can be estimated by the standard deviation of the measured amplitude timing value $\sigma_{t_{\mathrm{ATC}}}$ when the ATC is turned off and the corresponding sensitivity, according to (6). However as the obtained amplitude timing noise is in the range of an FPGA tick (i.e. 10 ns), quantization effects have to be taken into account. Assuming that the quantization is uncorrelated with the signal, the uncertainty model $\hat{U}$ and the measured uncertainty $\tilde{U}$ can be calculated by

$$\hat{U} = \sqrt{U^2 + \left(\frac{1}{S}\frac{\sigma_{\mathrm{qu}}}{\sigma_{\mathrm{I}}}\right)^2} \quad \text{and} \quad \tilde{U} = \frac{1}{S}\frac{\sigma_{t_{\mathrm{ATC}}}}{\sigma_{\mathrm{I}}}, \tag{14}$$

where S and U represent the original model while σ_{qu} and σ_{I} are fitting constants. Fig. 12 shows that the updated model matches the

Published version of the article: D. Brunner, S. Albert, F. Darrer, M. Hennecke, and G. Schitter, "Self-sensing control of resonant MEMS scanner by comb-drive current feedback", *Mechatronics*, vol. 78, 102631, 2021. DOI: 10.1016/j.mechatronics.2021.102631

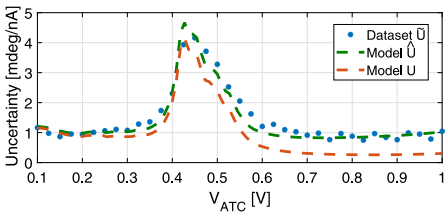

Fig. 12. Measured uncertainty obtained by analyzing the measured amplitude timing error when the ATC is turned off and a comparison to the proposed model. As the FPGA clock is limited, a uncertainty model is fitted that takes the timing quantization into account ($\sigma_{qu} = 11$ ns, $\sigma_I = 6.2$ nA).

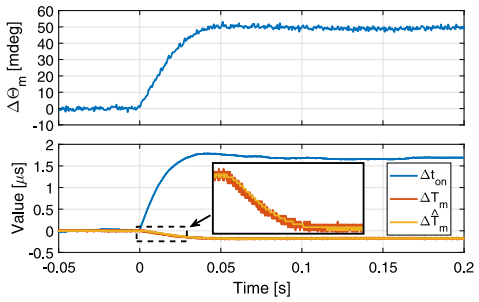

Fig. 13. Mirror amplitude response on a −100 ns set-point step of the ATC control loop ($\Theta_m = 13.75°$, $V_{ATC} = 0.8$ V). With the gains $G_{LP} = 0.125$, $G_P = 4$ and $G_I = 0.25$, the response shows an overdamped behavior and a fast settling time of < 50 ms. The variables with a Δ prefix only contain the deviation from the nominal operation point values.

data with good agreement while deviations occur as the assumption of uncorrelated quantization may not always be true, especially at such low errors. This shows that the timing quantization of the measured amplitude timing value due to the FPGA clock is directly influencing the achievable accuracy and precision of the amplitude measurement. To overcome this a time-to-digital converter (TDC) can be used especially for faster mirrors, allowing timing resolutions in the pico-second range.

Finally, the results suggest to use a low threshold voltage as it provides a high sensitivity while the measurement uncertainty is kept low. However in noisy environments the current signal curvature around the threshold crossing may cause a shift of the mean amplitude timing value, resulting in an amplitude change. If this cannot be compensated or avoided, a threshold between 0.6 V and 1 V should be chosen corresponding to approximately 45–70% of the maximum current signal value V_{I0} for the used operation point.

4.3. Verification of amplitude control

Fig. 13 shows the dynamic response on an ATC set-point step of −100 ns, resulting in 50 mdeg amplitude increase and a duty cycle reduction of 0.7%. The used mirror period filter gain $G_{LP} = 0.125$ provides accurate tracking of the mirror period while the noise is reduced as shown in the inset of the figure. The amplitude timing control gains $G_P = 4$ and $G_I = 0.25$, are set to achieve an overdamped behavior with a settling time of less than 50 ms for sudden external disturbance compensation. Fig. 14 shows the mirror amplitude deviation from the nominal operation point, when the amplitude timing control is turned

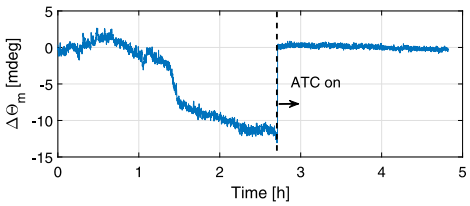

Fig. 14. Pointing error at maximum deflection of the desired operation point ($\Theta_m = 13.75°$, $V_{Supp} = 76$ V, $V_{ATC} = 0.8$ V) in an uncontrolled environment. Every 3 s one CCD frame is captured for the analysis. The mirror amplitude drifts due to environmental influences which is compensated when the ATC is turned on.

off at time zero and turned on again after about 2.7 h. The setup is placed in a room with an opened window, which allows no control of the ambient conditions of the MEMS mirror. The result shows that the amplitude drifts due to environmental variations such as temperature and pressure, as also shown in [6]. However the proposed ATC concept compensates the drift of −13 mdeg and keeps the MEMS mirror at the desired amplitude with a standard deviation of 0.26 mdeg. This corresponds to an optical pointing uncertainty of only 0.52 mdeg at the edges of a 55° field of view, while at the center 0.39 mdeg are achieved in measurements. Hence, the proposed system is 20 times better than the resolution requirement of 0.1° for a long range lidar as stated in [5] providing more than 10 000 pixels along the scan line with a precision of 10 sigma. Considering the driving speeds on highways the required detection range of hazardous objects for automotive lidars is 150 m [22], which can be detected with a resolution of about 14 mm by the proposed system. Furthermore the eDAsPLL correctly identified the scanning direction during all measurements by the proposed method.

In summary it is shown that the developed eDAsPLL can precisely control the MEMS mirror amplitude solely based on self-sensing comb-drive current feedback and simple circuitry. The mode coupling phenomenon that is implied by the lightweight MEMS mirror design using reinforcement structures allows the scanning direction detection, which would be otherwise not possible for out-of-plane comb-drives.

5. Conclusion

In this paper a simple high precision driving eDAsPLL for comb-drive actuated MEMS mirrors is proposed, utilizing the generated displacement current for phase, amplitude and scanning direction detection. The immediate phase compensation by asynchronous switching of the driving voltage allows fast tracking of the mirror movement while its amplitude is controlled by the duty cycle. The amplitude detection is based on the time between the summed current signal reaching a comparator threshold and the zero crossing of the mirror. The sensitivity and uncertainty are analyzed with respect to the chosen threshold level. The experimental results verify the analysis and show that a threshold between 45% and 70% of the maximum current signal value is preferable as it provides a good trade-off between sensitivity and uncertainty as well as drifts by measurement noise. The achieved optical pointing uncertainty of 0.52 mdeg at the edges of a 55° field of view allows 10 000 pixels with a precision of 10 sigma. It is found that the step towards lightweight MEMS mirror designs using reinforcement structures, to overcome performance limits, also allows the detection of the scanning direction by the difference in the left and right side comb-drive current, caused by a mode coupling phenomenon.

Published version of the article: D. Brunner, S. Albert, F. Darrer, M. Hennecke, and G. Schitter, "Self-sensing control of resonant MEMS scanner by comb-drive current feedback", *Mechatronics*, vol. 78, 102631, 2021. DOI: 10.1016/j.mechatronics.2021.102631

CRediT authorship contribution statement

David Brunner: Conceptualization, Methodology, Software, Validation, Formal analysis, Investigation, Writing – original draft, Visualization. **Stephan Albert:** Conceptualization, Methodology, Writing – review & editing. **Marcus Hennecke:** Conceptualization, Writing – review & editing. **Franz Darrer:** Conceptualization, Writing – review & editing. **Georg Schitter:** Conceptualization, Writing – review & editing, Supervision.

Declaration of competing interest

The authors declare that they have no known competing financial interests or personal relationships that could have appeared to influence the work reported in this paper.

Acknowledgments

This work has been supported in part by the Austrian Research Promotion Agency (FFG) under the scope of the LiDcAR project (FFG project number 860819).

The authors would like to thank Han Woong Yoo and Richard Schroedter for fruitful discussions.

References

[1] Hofmann U, Senger F, Janes J, Mallas C, Stenchly V, Wantoch T, et al. Wafer-level vacuum-packaged two-axis MEMS scanning mirror for pico-projector application. In: Proc. SPIE 8977. 2014.
[2] Xie H, Fedder G, Pan Y. MEMS-based endoscopic optical coherence tomography. In: Proc. SPIE 5721. 2005. p. 81–92.
[3] Hofmann U, Aikio M, Janes J, Senger F, Stenchly V, Weiss M, et al. Resonant biaxial 7-mm MEMS mirror for omnidirectional scanning. In: Proc. SPIE 8616. 2013. p. 71–84.
[4] Yoo HW, Druml N, Brunner D, Schwarzl C, Thurner T, Hennecke M, et al. Mems-based lidar for autonomous driving. Elektrotech Inftech 2018;135(6):408–15.
[5] Druml N, Maksymova I, Thurner T, Lierop D, Hennecke M, Foroutan A. 1D MEMS micro-scanning LiDAR. In: Int. conf. on sensor device technologies and appl. 2018.
[6] Tortschanoff A, Lenzhofer M, Frank A, Wildenhain M, Sandner T, Schenk H, et al. Optical position feedback and phase control of MOEMS scanner mirrors. In: Proc. SPIE 7594. 2010. p. 168–178.
[7] Ataman C, Urey H. Modeling and characterization of comb-actuated resonant microscanners. J Micromech Microeng 2005;16(1):9–16.
[8] Grahmann J, Graßhoff T, Conrad H, Sandner T, Schenk H. Integrated piezoresistive position detection for electrostatic driven micro scanning mirrors. In: Proc. SPIE 7930. 2011. p. 260–67.
[9] Baran U, Brown D, Holmstrom S, Balma D, Davis WO, Muralt P, et al. Resonant PZT MEMS scanner for high-resolution displays. J Microelectromech Syst 2012;21:1303–10.
[10] Xia C, Qiao D, Zhang Y, Su X, Guo Z. A position feedback solution based on the acoustic signal produced by electrostatically driven MEMS scanning mirror. In: IEEE-NEMS. 2017. p. 558–61.
[11] Roscher K-U, Fakesch U, Schenk H, Lakner HK, Schlebusch D. Driver ASIC for synchronized excitation of resonant micromirrors. In: Proc. SPIE 4985. 2003. p. 121–30.
[12] Chemmanda LJ, Jianrong CC, Singh RP, Roterman Y. ASIC front-end for sensing MEMS-mirror position. In: International symposium on integrated circuits. 2014. p. 396–99.
[13] Dooyoung Hah, Patterson PR, Nguyen HD, Toshiyoshi H, Wu MC. Theory and experiments of angular vertical comb-drive actuators for scanning micromirrors. IEEE J Sel Top Quantum Electron 2004;10(3):505–13.
[14] Brunner D, Yoo HW, Schitter G. Precise phase control of resonant MOEMS mirrors by comb-drive current feedback. Mechatronics 2020;71:102420.
[15] Brunner D, Yoo HW, Thurner T, Schitter G. Data based modelling and identification of nonlinear SDOF MOEMS mirror. In: Proc. SPIE 10931. 2019. p. 269–78.
[16] Farrugia R, Grech I, Camilleri D, Casha O, Gatt E, Micallef J. Theoretical and finite element analysis of dynamic deformation in resonating micromirrors. Microsyst Technol 2017;24:1–11.
[17] Nee J, Conant R, Muller R, Lau K. Lightweight, optically flat micromirrors for fast beam steering. In: IEEE/LEOS int. conf. on opt. MEMS (Cat. No.00EX399). 2000. p. 9–10.
[18] Hsu S, Klose T, Drabe C, Schenk H. Fabrication and characterization of a dynamically flat high resolution micro-scanner. J Opt A: Pure Appl Opt 2008;10(4):044005.
[19] Yoo HW, Riegler R, Brunner D, Albert SG, Thurner T, Schitter G. Experimental evaluation of vibration influence on a resonant MEMS scanning system for automotive lidars. IEEE Trans Ind Electron 2021;1.
[20] Brunner D, Yoo HW, Schitter G. Linear modeling and control of comb-actuated resonant MEMS mirror with nonlinear dynamics. IEEE Trans Ind Electron 2021;68(4):3315–23.
[21] Shahid W, Qiu Z, Duan X, Li H, Wang TD, Oldham KR. Modeling and simulation of a parametrically resonant micromirror with duty-cycled excitation. J Microelectromech Syst 2014;23(6):1440–53.
[22] Royo S, Ballesta-Garcia M. An overview of lidar imaging systems for autonomous vehicles. Appl Sci 2019;9(19):4093.

David Brunner is Ph.D. student at the Automation and Control Institute (ACIN) of TU Wien. He received his M.Sc. degree in Energy Systems and Automation Technology from TU Wien, Austria, in 2017. His primary research interests include advanced identification and control concepts, high performance mechatronic systems and system integration.

Stephan Albert received the M.A. degree as a Fulbright Scholar from Stony Brook University in 2007, the Diploma degree from TU Munich in 2010, and the Ph.D. degree in physics from TU Munich in 2015. He is currently a Principal Engineer of MEMS devices with Infineon Technologies AG, Neubiberg, Germany. He has worked experimentally in the fields of quantum optics, ultracold atoms, and magnetism and theoretically in the field of many-body physics. At Infineon, he is responsible for the design, modeling, and the development of integration concepts for MEMS devices, such as pressure sensors, accelerometers, and scanning mirror devices.

Marcus Hennecke (male) studied Electrical Engineering at the Technical University of Darmstadt from 1986, completing his studies in 1991 with a Diploma degree. In 1992 he graduated from Stanford University with a Master of Science degree in the area of neural networks and continued as doctoral student on the topic of computer aided lip reading. In 1996 he completed his thesis and moved to Ulm in Germany where he worked on an automated spoken language translator at the Daimler-Benz research center until 1998. In the years to come until 2006 he worked on automated speech recognition for automotive dialog systems for the companies Daimler-Benz Aerospace AG, TEMIC Telefunken and Harman Becker as head of the departments algorithms, research and speech recognition, respectively. In 2006 he then moved to Graz where he headed the business segment Pattern Recognition and Image Processing (PRIP) at the Biometric Center of Siemens until 2009.

Between 2009 and 2016 he worked for EFKON AG as head of the departments Frontend and Machine Vision. Since November 2016 Mr. Hennecke is with the Design Center Graz of Infineon Technologies where he is responsible for Innovation&Funding Management. In his professional career Mr. Hennecke has initiated and executed various successful national (German and Austrian) as well as European funded projects. He is (co-)author of numerous publications and patents.

Published version of the article: D. Brunner, S. Albert, F. Darrer, M. Hennecke, and G. Schitter, "Self-sensing control of resonant MEMS scanner by comb-drive current feedback", *Mechatronics*, vol. 78, 102631, 2021. DOI: 10.1016/j.mechatronics.2021.102631

Franz Darrer studied Electrical Engineering at the Technical University in Graz. He conducted his diploma thesis about CMOS Op-Amps at EZM Siemens in Villach. In 1991 he completed his studies with a Diploma degree. From 1992 to 1998 he worked at Austria Micro Systems on RF receivers, PLLs, DLLs and RAMs. In 1998 he joined the Design Center Graz of Siemens, later Infineon, where he initially worked on TV tuners, bipolar and CMOS RF transmitters, currently on Flash memories, TPMS systems, and an ISO26262-conform control ASIC of an oscillating MEMS mirror for laser scanners. He is (co)inventor of several patents.

Georg Schitter is Professor for Advanced Mechatronic Systems at the Automation and Control Institute (ACIN) of TU Wien. He received an M.Sc. in Electrical Engineering from TU Graz, Austria (2000) and an M.Sc. and Ph.D. degree from ETH Zurich, Switzerland (2004).

His primary research interests are on high-performance mechatronic systems, particularly for applications in the high-tech industry, scientific instrumentation, and mechatronic imaging systems, such as AFM, scanning laser and LIDAR systems, telescope systems, adaptive optics, and lithography systems for semiconductor industry. He received the journal best paper award of IEEE/ASME Transactions on Mechatronics (2017), of the IFAC Mechatronics (2008–2010), of the Asian Journal of Control (2004–2005), and the 2013 IFAC Mechatronics Young Researcher Award. He served as an Associate Editor for IFAC Mechatronics, Control Engineering Practice, and for the IEEE Transactions on Mechatronics.

Published version of the article: D. Brunner, S. Albert, F. Darrer, M. Hennecke, and G. Schitter, "Self-sensing control of resonant MEMS scanner by comb-drive current feedback", *Mechatronics*, vol. 78, 102631, 2021. DOI: 10.1016/j.mechatronics.2021.102631